ACS Macro Letters

Letter

pubs.acs.org/macroletters

Monodisperse Low-Bandgap Macromolecule-Based 5,5′-Bibenzo[c][1,2,5]thiadiazole Swivel Cruciform for Organic Solar Cells

Debin Ni,[†] Baofeng Zhao,[‡] Ting Shi,[†] Shuying Ma,[†] Guoli Tu,*[,†] and Hongbin Wu*[,‡]

[†]School of Optical and Electronic Information, Wuhan National Laboratory for Optoelectronics, Huazhong University of Science and Technology, Wuhan 430074, P. R. China

[‡]Institute of Polymer Optoelectronic Materials and Devices, State Key Laboratory of Luminescent Materials and Devices, South China University of Technology, Guangzhou 510640, P. R. China

Supporting Information

ABSTRACT: A novel low bandgap star-like macromolecule was synthesized and applied as electron donor material in the bulk heterojunction solar cells, in which the 5,5′-bibenzo[c]-[1,2,5]thiadiazole was used as the central node, in conjunction with four conjugated donor−acceptor arms. Compared with the corresponding small molecule with first generation arms, the macromolecule with second generation branches exhibited significantly enhanced photovoltaic device performances (blended with PC71BM as the active layer) due to dramatically improved short-circuit current density (J_{sc}) and fill factor (FF). The improvement in J_{sc} and FF can be attributed to the more broad absorption and the more favorable phase separation when comparing a monodisperse macromolecule with the second generation arms (SFTBT) with a small molecule with first generation branches (DFTBT).

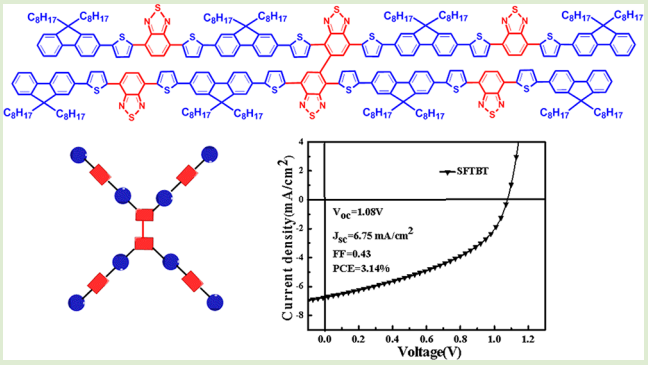

Recently, organic photovoltaics (OPVs) have been extensively studied for an alternative clean energy source because of their unique advantages, such as low-cost fabrication, good flexibility, light weight, and compatibility with cheap roll-to-roll processing techniques. In general, the active layer is based on a blend of a semiconducting polymer/small molecule and a fullerene derivative, which behave as the electron donor and acceptor, respectively.[1−18] To date, the power conversion efficiency of the state-of-the-art OPVs based on polymers as the donor material has reached 9.2% in the scientific literature.[19] In spite of their superior film-forming properties, polymer materials tend to suffer from problems such as molecular weight polydispersity, weak batch-to-batch reproducibility, and end group variation, all of which could cause a strong impact on the performance of devices and are extremely difficult to control during the polymer synthesis process. In contrast with polymers, small molecular materials possess well-defined structures and can provide completely reproducible performance. We note that rapid progress has been achieved in the development of small molecules for OPVs, resulting in high efficiency over 7.8%.[20−23] On the other side, small molecular electron donor materials have a strong tendency to crystallize at elevated temperature, which will result in an overlarge donor domain environment and unfavorable phase separation for electron transfer between the donor/acceptor interface.[24] In addition, the crystallized films of small molecules may exhibit relatively poor mechanical properties when compared with polymer counterparts, which is a fatal shortcoming for the flexible solar cell applications.

Monodisperse macromolecules such as conjugated dendrimers, which combine the advantages of polymers and small molecule optoelectronic materials, have been successfully studied and applied in organic light-emitting devices (OLEDs).[25−31] These compounds exhibit well-defined chemical structure and excellent mechanical properties and can be purified to the level of that of small molecules when following the same purification process. This kind of macromolecular material can have excellent solubility in organic solvents, thus is readily suitable for solution processing including spin-casting or inkjet printing. For instance, Ma et al. demonstrated the use of thiophene-centered dendrimers as donor materials for OPVs.[32] They synthesized a dendritic oligothiophene-based macromolecule containing 90 thiophene units and explored their photovoltaic properties. When blended with PCBM and used as the active layer, the obtained device showed a power conversion efficiency (PCE) of 1.72%, which was lower than that of P3HT/PCBM because of its less efficient absorption and lower charge mobility as a result of a large amount of branches that will lead to disorder in the intermolecular stacking in films. Therefore, to make use of the donor for highly efficient OPVs, development of new material design strategies

Received: May 15, 2013
Accepted: June 24, 2013
Published: June 26, 2013

   dx.doi.org/10.1021/mz4002436 | ACS Macro Lett. 2013, 2, 621−624

Scheme 1. Chemical Structures of SFTBT and DFTBT

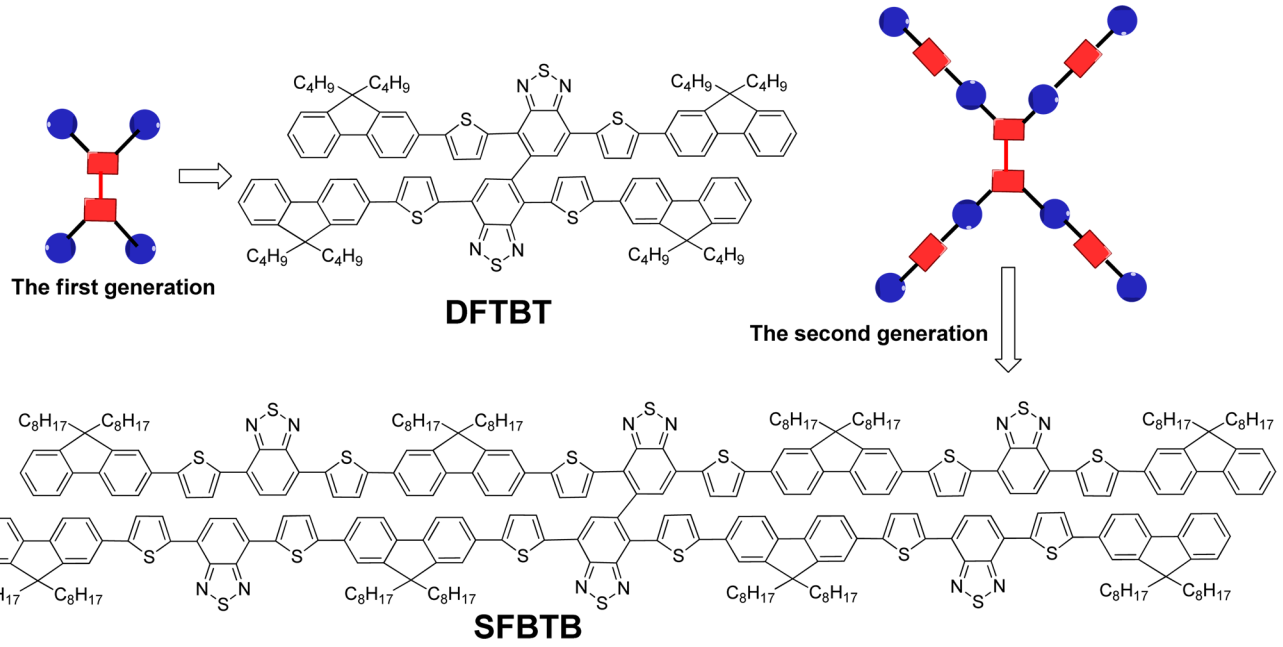

that can enable intermolecular stacking and improve light absorption is in urgent need.

Here we report the synthesis of star-like macromolecular donor material with four alternate donor−acceptor branches which can enhance light absorption and intermolecular stacking for photovoltaic applications. A swivel cruciform structure with tetra arms was selected as the framework of the macromolecule for the reason that the swivel cruciform small molecule has been proved to be efficient for organic filed-effect transistors and OPVs.[33−36] On the basis of the consideration that benzo[c][1,2,5]thiadiazole was widely used as building blocks in efficient donor materials,[37−40] 5,5′-bibenzo[c][1,2,5]-thiadiazole was chosen as the central unit in this study. Two low bandgap donor materials, including a small molecule with first generation branches (DFTBT) and a monodisperse macromolecule with the second generation arms (SFTBT), were prepared to investigate the influence of extended conjugated arms on their physical properties and the corresponding OPV device performances. The chemical structures of DFTBT and SFTBT are shown in Scheme 1.

DFTBT and SFTBT were synthesized by a standard Stille condensation reaction with yield of 64% and 45%, respectively. The synthetic procedures of DFTBT and SFTBT were shown in the Supporting Information (S1). Their structures have been proved by NMR and time-resolved mass spectrometry. SFTBT can be fine purified by column chromatography as a small molecule and shows excellently solubility in chloroform, toluene, and so on, although its molecular weight has reached 4896. Considering the poor solubility of the corresponding linear polymer with similar molecular weight, the good solubility can be attributed to the swivel cruciform core of SFTBT. The thermal stability of DFTBT and SFTBT was investigated by thermogravimetric analysis (TGA), showing a 5% weight loss at 415 and 423 °C, respectively. Thermal properties of DFTBT and SFTBT were also determined by differential scanning calorimetry (DSC). Compared with SFTBT (T_g = 82 °C), a shorter alkyl chain on the 9-position of fluorene units was applied to DFTBT to improve its T_g of 111 °C. The absorption spectra of DFTBT and SFTBT in solution and film are presented in Figure 1. The absorptivity of

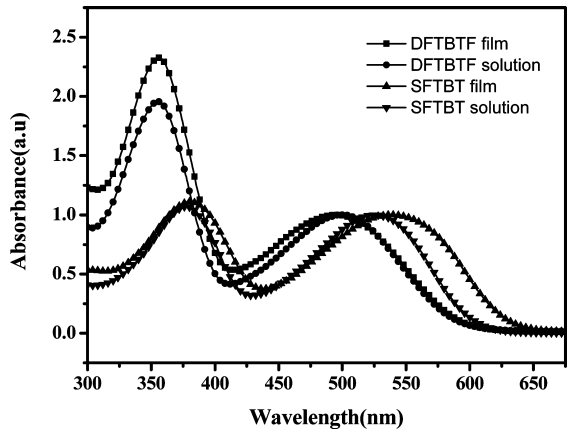

Figure 1. UV−vis absorption spectrum of SFTBT and DFTBT in toluene solution and as spin-coated at 298 K.

the two materials in solution is shown in Figure S1 (Supporting Information), and the detailed data are shown in Table 1. DFTBT shows maximum absorption peaks (λ_{max}) of 495 and 499 nm in the solution and film, respectively, indicating the weak intermolecular interaction in the DFTBT solid state. The as-cast film of SFTBT from toluene solution (10 mg/mL) shows a λ_{max} at 538 nm, which exhibits a red shift λ_{max} of 13 nm compared to that in solution, suggesting the existence of intermolecular stacking in the solid state. Compared with DFTBT, SFTBT exhibits approximately a 40 nm red shift in film due to intermolecular aggregation in the solid state. The absorption cutoff of DFTBT and SFTBT is 600 and 630 nm, corresponding to a bandgap of 2.06 and 1.97 eV, respectively. The electrochemical properties of DFTBT and SFTBT were investigated by circular voltammetry (CV) with Ag/Ag+ (0.1 M $AgNO_3$ in acetonitrile) as the reference electrode, which was calibrated to be −4.74 eV against the ferrocene/ferrocenium

dx.doi.org/10.1021/mz4002436 | ACS Macro Lett. 2013, 2, 621−624

Table 1. Summary of the Optical and Electrochemical Properties of the SFTBT and DFTBT and Device Parameters of the OPVs Based on These Compounds, Tested under an AM 1.5 G Solar Simulator (100 mW/cm^2)

compound	M_z	Abs ε (mol^{-1} cm^{-1})	λ_{max} (nm) film	$E_{g,opt}$[a]	HOMO[b,c] (eV)	LUMO[b,c] (eV)	$E_{g,elec}$[d]	V_{oc} (V)	J_{sc} (mA/cm^2)	FF	PCE (%)
DFTBT	1704	495(4.8 × 10^3)	499	2.06	−5.39	−3.44	1.95	1.09	2.47	0.27	0.74
SFTBT	4896	525(2.5 × 10^4)	538	1.97	−5.39	−3.43	1.96	1.08	6.75	0.43	3.14

[a]Optical energy gap determined from the onset position of the absorption band. [b,c]HOMO and LUMO position (vs vacuum) determined from onset of oxidation and reduction. [d]Electrochemical energy gap.

(Fc/Fc+) redox couple calculated from the onset of oxidation and reduction, the HOMO and LUMO levels of SFTBT were −5.39 and −3.43 eV, respectively, indicating an electrochemical bandgap of 1.96 eV and agreeing well with the resulting bandgap of its UV spectrum. The cyclic voltammograms of two materials are shown in Figure S2 (Supporting Information). The HOMO and LUMO levels of DFTBT were almost the same as SFTBT, originating from the same molecule skeleton. The low-lying HOMO energy levels of DFTBT and SFTBT provide the necessary characteristics for large V_{oc} in the devices.

Photovoltaic devices were fabricated by spin-coating from chlorobenzene solution with $PC_{71}BM$ ([6,6]-phenyl-C_{71}-butyric acid methylester) as the acceptor in a conventional structure of ITO/PEDOT:PSS (30 nm)/DFTBT or SFTBT:$PC_{71}BM$ (1:3, w/w, 90 nm)/Ca (15 nm)/Al (100 nm). The current density versus applied voltage curve (J–V characteristics) of the resulting device under AM 1.5G illumination was shown in Figure 2, and the deduced

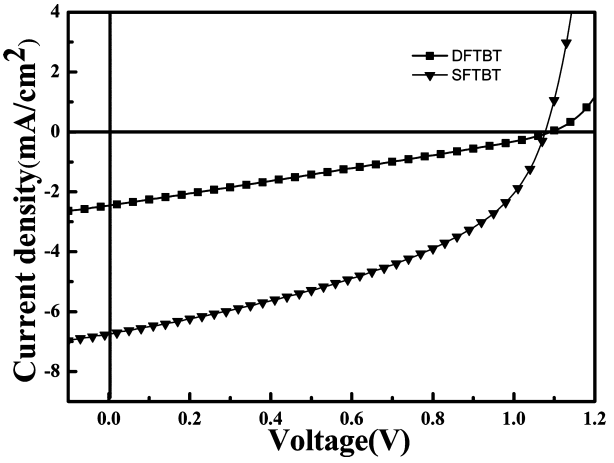

Figure 2. Current density–voltage (J–V) curves of the solar cells based on SFTBT:$PC_{71}BM$ (1:3, w/w) and DFTBT:$PC_{71}BM$ (1:3, w/w) under AM 1.5G simulated solar illumination (100 mW/cm^2).

parameters were summarized in Table 1, respectively. The DFTBT-based device exhibited a large V_{oc} (open-circuit voltage) of 1.09 V. However, limited by the low short-circuit current density (J_{sc}) of 2.47 mA/cm^2, the low fill factor (FF) of 27% and a low PCE of 0.74% was obtained. It is worthy to note that the SFTBT device showed a significant efficiency of 3.14% with a V_{oc} of 1.08 V, J_{sc} of 6.75 mA/cm^2, and FF of 43%, respectively. Figure 3 depicted the incident photon to current efficiency (IPCE) curve of DFTBT and SFTBT devices, in which the SFTBT device exhibits a broad photoresponse covering the entire visible region between 350 and 750 nm, with a maximum of 49.6% at 525 nm, while the DFTBT device shows a maximum of 18% at 520 nm, much lower than that of SFTBT. The observed significant difference in photoresponse between the DFTBT and SFTBT device can be attributed to

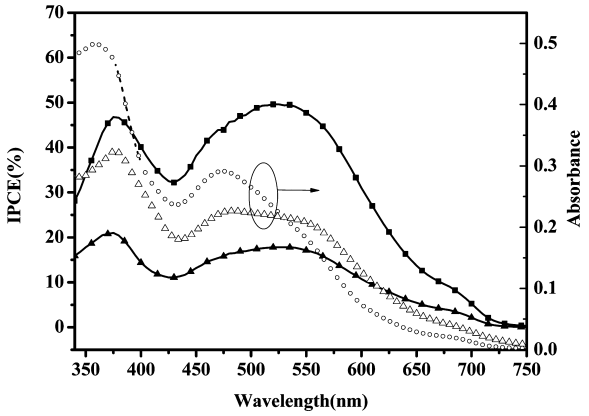

Figure 3. Incident photon to current efficiency (IPCE) curve of DFTBT and SFTBT devices.

the absorption of the active layer (Figure 3) and the relatively large domain phase separation, as indicated by atomic force microscopy (AFM) phase images of films of the blend of DFTBT and SFTBT with $PC_{71}BM$ (1:3, w/w) (see Figure S3, Supporting Information).

In summary, we have successfully developed low bandgap star-like macromolecules and investigated the influence of extended conjugated branches on its optical properties and intermolecular stacking. Compared with the counterpart small molecule, the extended branches of arms in the macromolecule dramatically improved its intermolecular stacking, thus broadening absorption, without alternating the HOMO and LUMO energy levels. When $PC_{71}BM$ was chosen as the electron acceptor, the obtained OPVs based on this macromolecule showed 2.5 times that of the small molecule in J_{sc}, mainly due to the improved absorption and optimized nanophase separation in the blended film. In conjunction with a much improved FF (about 60% higher than that of the small molecule), the macromolecule-based devices resulted in a PCE of 3.14%, which is much higher than that of the device from the small molecule. The results demonstrated in the study clearly indicated that this kind of macromolecule can be a promising material for photovoltaic applications.

■ ASSOCIATED CONTENT

Supporting Information

Experimental procedures, synthesis of monomers, cyclic voltammograms, and AFM images are included. This material is available free of charge via the Internet at http://pubs.acs.org.

■ AUTHOR INFORMATION

Corresponding Author

*E-mail: tgl@mail.hust.edu.cn; hbwu@scut.edu.cn.

Notes

The authors declare no competing financial interest.

■ ACKNOWLEDGMENTS

We thank the financial support by National Natural Science Foundation of China (nos. 51073063, 21274048, 20834005, and 51225301).

■ REFERENCES

(1) Tang, C. W. *Appl. Phys. Lett.* **1986**, *48* (2), 183−185.
(2) Yu, G.; Gao, J.; Hummelen, J. C.; Wudl, F.; Heeger, A. J. *Science* **1995**, *270* (5243), 1789−1791.
(3) Li, G.; Shrotriya, V.; Huang, J.; Yao, Y.; Moriarty, T.; Emery, K.; Yang, Y. *Nat. Mater.* **2005**, *4* (11), 864−868.
(4) Ma, W.; Yang, C.; Gong, X.; Lee, K.; Heeger, A. J. *Adv. Funct. Mater.* **2005**, *15* (10), 1617−1622.
(5) Kim, Y.; Cook, S.; Tuladhar, S. M.; Choulis, S. A.; Nelson, J.; Durrant, J. R.; Bradley, D. D. C.; Giles, M.; McCulloch, I.; Ha, C.-S.; Ree, M. *Nat. Mater.* **2006**, *5* (3), 197−203.
(6) Blouin, N.; Michaud, A.; Leclerc, M. *Adv. Mater.* **2007**, *19* (17), 2295−2300.
(7) Kim, J. Y.; Lee, K.; Coates, N. E.; Moses, D.; Nguyen, T.-Q.; Dante, M.; Heeger, A. J. *Science* **2007**, *317* (5835), 222−225.
(8) Peet, J.; Kim, J. Y.; Coates, N. E.; Ma, W. L.; Moses, D.; Heeger, A. J.; Bazan, G. C. *Nat. Mater.* **2007**, *6* (7), 497−500.
(9) Liang, Y.; Wu, Y.; Feng, D.; Tsai, S.-T.; Son, H.-J.; Li, G.; Yu, L. *J. Am. Chem. Soc.* **2008**, *131* (1), 56−57.
(10) Chen, H.-Y.; Hou, J.; Zhang, S.; Liang, Y.; Yang, G.; Yang, Y.; Yu, L.; Wu, Y.; Li, G. *Nat. Photonics* **2009**, *3* (11), 649−653.
(11) Walker, B.; Tamayo, A. B.; Dang, X.-D.; Zalar, P.; Seo, J. H.; Garcia, A.; Tantiwiwat, M.; Nguyen, T.-Q. *Adv. Funct. Mater.* **2009**, *19* (19), 3063−3069.
(12) Piliego, C.; Holcombe, T. W.; Douglas, J. D.; Woo, C. H.; Beaujuge, P. M.; Fréchet, J. M. J. *J. Am. Chem. Soc.* **2010**, *132* (22), 7595−7597.
(13) Li, Z.; Ding, J.; Song, N.; Lu, J.; Tao, Y. *J. Am. Chem. Soc.* **2010**, *132* (38), 13160−13161.
(14) Lee, O. P.; Yiu, A. T.; Beaujuge, P. M.; Woo, C. H.; Holcombe, T. W.; Millstone, J. E.; Douglas, J. D.; Chen, M. S.; Fréchet, J. M. J. *Adv. Mater.* **2011**, 5359−5363.
(15) Price, S. C.; Stuart, A. C.; Yang, L.; Zhou, H.; You, W. *J. Am. Chem. Soc.* **2011**, *133* (12), 4625−4631.
(16) Amb, C. M.; Chen, S.; Graham, K. R.; Subbiah, J.; Small, C. E.; So, F.; Reynolds, J. R. *J. Am. Chem. Soc.* **2011**, *133* (26), 10062−10065.
(17) Lin, Y.; Zhang, Z.-G.; Bai, H.; Li, Y.; Zhan, X. *Chem. Commun.* **2012**, *48* (77), 9655−9657.
(18) Sun, Y.; Welch, G. C.; Leong, W. L.; Takacs, C. J.; Bazan, G. C.; Heeger, A. J. *Nat. Mater.* **2012**, *11* (1), 44−48.
(19) He, Z.; Zhong, C.; Su, S.; Xu, M.; Wu, H.; Cao, Y. *Nat. Photonics* **2012**, *6* (9), 591−595.
(20) Li, Z.; He, G.; Wan, X.; Liu, Y.; Zhou, J.; Long, G.; Zuo, Y.; Zhang, M.; Chen, Y. *Adv. Energy Mater.* **2012**, *2* (1), 74−77.
(21) Sun, Y.; Welch, G. C.; Leong, W. L.; Takacs, C. J.; Bazan, G. C.; Heeger, A. J. *Nat. Mater.* **2012**, *11* (1), 44−48.
(22) Zhou, J.; Wa. n, X.; Liu, Y.; Zuo, Y.; Li, Z.; He, G.; Long, G.; Ni, W.; Li, C.; Su, X.; Chen, Y. *J. Am. Chem. Soc.* **2012**, *134* (39), 16345−16351.
(23) Kyaw, A. K. K.; Wang, D. H.; Gupta, V.; Zhang, J.; Chand, S.; Bazan, G. C.; Heeger, A. J. *Adv. Mater.* **2013**, 2397−2402.
(24) Blom, P. W. M.; Mihailetchi, V. D.; Koster, L. J. A.; Markov, D. E. *Adv. Mater.* **2007**, *19* (12), 1551−1566.
(25) Liu, J.; Cheng, Y.; Xie, Z.; Geng, Y.; Wang, L.; Jing, X.; Wang, F. *Adv. Mater.* **2008**, *20* (7), 1357−1362.
(26) Lo, S.-C.; Burn, P. L. *Chem. Rev.* **2007**, *107* (4), 1097−1116.
(27) Hwang, S.-H.; Moorefield, C. N.; Newkome, G. R. *Chem. Soc. Rev.* **2008**, *37* (11), 2543−2557.
(28) Ding, J.; Zhang, B.; Lü, J.; Xie, Z.; Wang, L.; Jing, X.; Wang, F. *Adv. Mater.* **2009**, *21* (48), 4983−4986.
(29) Lai, W.-Y.; Xia, R.; He, Q.-Y.; Levermore, P. A.; Huang, W.; Bradley, D. D. C. *Adv. Mater.* **2009**, *21* (3), 355−360.
(30) Nguyen, T.-T.-T.; Türp, D.; Wang, D.; Nölscher, B.; Laquai, F.; Müllen, K. *J. Am. Chem. Soc.* **2011**, *133* (29), 11194−11204.
(31) Chen, L.; Li, P.; Cheng, Y.; Xie, Z.; Wang, L.; Jing, X.; Wang, F. *Adv. Mater.* **2011**, *23* (26), 2986−2990.
(32) Ma, C.-Q.; Fonrodona, M.; Schikora, M. C.; Wienk, M. M.; Janssen, R. A. J.; Bäuerle, P. *Adv. Funct. Mater.* **2008**, *18* (20), 3323−3331.
(33) Zen, A.; Bilge, A.; Galbrecht, F.; Alle, R.; Meerholz, K.; Grenzer, J.; Neher, D.; Scherf, U.; Farrell, T. *J. Am. Chem. Soc.* **2006**, *128* (12), 3914−3915.
(34) Xue, S.; Liu, S.; He, F.; Yao, L.; Gu, C.; Xu, H.; Xie, Z.; Wu, H.; Ma, Y. *Chem. Commun.* **2013**, *49*, 5730−5732.
(35) Wright, I. A.; Kanibolotsky, A. L.; Cameron, J.; Tuttle, T.; Skabara, P. J.; Coles, S. J.; Howells, C. T.; Thomson, S. A. J.; Gambino, S.; Samuel, I. D. W. *Angew. Chem., Int. Ed.* **2012**, *51* (19), 4562−4567.
(36) Ma, S.; Fu, Y.; Ni, D.; Mao, J.; Xie, Z.; Tu, G. *Chem. Commun.* **2012**, *48* (97), 11847−11849.
(37) Qin, R.; Li, W.; Li, C.; Du, C.; Veit, C.; Schleiermacher, H.-F.; Andersson, M.; Bo, Z.; Liu, Z.; Inganäs, O.; Wuerfel, U.; Zhang, F. *J. Am. Chem. Soc.* **2009**, *131* (41), 14612−14613.
(38) Chen, Y.-H.; Lin, L.-Y.; Lu, C.-W.; Lin, F.; Huang, Z.-Y.; Lin, H.-W.; Wang, P.-H.; Liu, Y.-H.; Wong, K.-T.; Wen, J.; Miller, D. J.; Darling, S. B. *J. Am. Chem. Soc.* **2012**, *134* (33), 13616−13623.
(39) Xu, Y.-X.; Chueh, C.-C.; Yip, H.-L.; Ding, F.-Z.; Li, Y.-X.; Li, C.-Z.; Li, X.; Chen, W.-C.; Jen, A. K. Y. *Adv. Mater.* **2012**, *24* (47), 6356−6361.
(40) Hou, J.; Chen, H.-Y.; Zhang, S.; Li, G.; Yang, Y. *J. Am. Chem. Soc.* **2008**, *130* (48), 16144−16145.